Genome-wide association analyses identify two novel susceptibility loci for pachychoroid disease central serous chorioretinopathy

Yoshikatsu Hosoda[1,2], Masahiro Miyake[1,2*], Rosa L. Schellevis[3], Camiel J.F. Boon[4], Carel B Hoyng[3], Akiko Miki[5], Akira Meguro[6], Yoichi Sakurada[7], Yoneyama Seigo[7], Yukari Takasago[8], Masayuki Hata[1], Yuki Muraoka[1], Hideo Nakanishi[1], Akio Oishi[1], Sotaro Ooto[1], Hiroshi Tamura[1], Akihito Uji[1], Manabu Miyata[1], Ayako Takahashi[1], Naoko Ueda-Arakawa[1], Atsushi Tajima[9], Takehiro Sato[9], Nobuhisa Mizuki[6], Chieko Shiragami[8], Tomohiro Iida[10], Chiea Chuen Khor[11,12], Tien Yin Wong[11,13,14], Ryo Yamada[2], Shigeru Honda[5,15], Eiko K. de Jong[3], Anneke I. den Hollander[3], Fumihiko Matsuda[2], Kenji Yamashiro[1,16†], & Akitaka Tsujikawa[1†]

[1]Department of Ophthalmology and Visual Sciences, Kyoto University Graduate School of Medicine, Kyoto, Japan

[2]Center for Genomic Medicine, Kyoto University Graduate School of Medicine, Kyoto, Japan

[3]Department of Ophthalmology, Donders Institute of Brain, Cognition and Behaviour, Radboud University Medical Centre, Nijmegen, the Netherlands

[4]Department of Ophthalmology, Leiden University Medical Center, Leiden, the Netherlands

[5]Department of Surgery, Division of Ophthalmology, Kobe University Graduate School of Medicine, Kobe, Japan

[6]Department of Ophthalmology and Visual Sciences, Yokohama City University School of Medicine, Yokohama, Japan

[7]Department of Ophthalmology, University of Yamanashi, Faculty of Medicine, Yamanashi, Japan

[8]Department of Ophthalmology, Kagawa University Faculty of Medicine, Kagawa, Japan

[9]Department of Bioinformatics and Genomics, Graduate School of Advanced Preventive Medical Sciences, Kanazawa University, Kanazawa, Ishikawa, Japan

[10]Department of Ophthalmology, Tokyo Women's Medical University, Tokyo, Japan

[11]Singapore National Eye Centre, Singapore Eye Research Institute, Singapore

[12]Division of Human Genetics, Genome Institute of Singapore, Singapore

[13]Saw Swee Hock School of Public Health, National University of Singapore and National University Health System, Singapore

[14]Ophthalmology and Visual Sciences Academic Clinical Program, Duke-NUS Medical School, National University of Singapore, Singapore

[15]Department of Ophthalmology and Visual Sciences, Osaka City University Graduate School of Medicine, Osaka, Japan

[16]Department of Ophthalmology, Otsu Red-Cross Hospital, Otsu, Japan

† These authors jointly directed this work.

Corresponding author:

[*]Masahiro Miyake, M.D., Ph.D. (Kyoto Univ.), M.P.H. (Harvard)

Department of Ophthalmology and Visual Sciences

Kyoto University Graduate School of Medicine

54 Shogoin, Kawahara, Sakyo, Kyoto 606-8507, Japan

Abstract

The recently emerged pachychoroid concept has changed the understanding of age-related macular degeneration (AMD) which is a major cause of blindness; recent studies attributed AMD in part to pachychoroid disease central serous chorioretinopathy (CSC), suggesting the importance of elucidating the CSC pathogenesis. Our large genome-wide association study followed by validation studies in three independent Japanese and European cohorts, consisting of 1,546 CSC samples and 13,029 controls, identified two novel CSC susceptibility loci: *TNFRSF10A-LOC389641* and near *GATA5* (rs13278062, odds ratio = 1.35, $P = 1.26 \times 10^{-13}$; rs6061548, odds ratio = 1.63, $P = 5.36 \times 10^{-15}$). A T allele at *TNFRSF10A-LOC389641* rs13278062, a risk allele for CSC, is known to be a risk allele for AMD. This study not only identified new susceptibility genes for CSC, but also improves the understanding of the pathogenesis of AMD.

Introduction

Central serous chorioretinopathy (CSC) is a common eye disease characterized by serous retinal detachment of the macular regions and retinal pigment epithelium (RPE).[1,2] Although retinal detachments in CSC eyes typically resolve spontaneously, some cases become chronic resulting in permanent retinal tissue damage.[3–5] Additionally, recent studies have shown that the occurrence of choroidal neovascularization (CNV) is a common complication leading to severe vision loss.[6,7] Based on these findings, CSC is currently recognized as an important sight-threatening disease that can lead to legal blindness. Although clinical studies have shown that dysfunction of the retinal pigment epithelium and hyperpermeability of the choroidal vessels are essential in the etiology of CSC,[8] the exact mechanisms underlying CSC pathology remain unknown. Previous studies reported that the risk factors of CSC include glucocorticoid use, increased adrenergic hormones, stress, male gender, *Helicobacter pylori* infection, and type A personality.[1,5,9–16]

Recently, the pathological overlap between age-related macular degeneration (AMD), which is a major cause of legal blindness in developed countries, and CSC has received increased attention as they share similar clinical characteristics, including serous retinal detachment, pigment epithelium detachment, and CNV occurrence. Particularly, because CNV secondary to CSC (which was recently named as pachychoroid neovasculopathy because of its characteristic thick ["pachy-"] choroid[17–19]) often masquerades as AMD,[20] recent studies highlighted the importance of differentiating AMD and CSC.[18,19,21–25] Interestingly, although AMD and CSC show similar clinical manifestations, genetic studies revealed that they have contrasting characteristics with respect to c*omplement factor H* (*CFH*), an established AMD susceptibility gene;[26] the risk alleles for AMD at *CFH* Y402H and *CFH* I62V confer a protective effect against CSC.[27–29] Taken together, investigating the genetic background of

CSC is currently of great importance and can improve the understanding of the etiology of both CSC and AMD.

Two genome-wide association studies (GWASs) for CSC have been reported.[30,31] However, both studies have limitations such as a lack of replication studies using independent cohorts and limited sample sizes. Even after considering previous candidate gene studies,[28,32–34] no CSC susceptibility gene other than *CFH* has been well-replicated and established. Therefore, robust GWASs are needed to further understand the genetic background of CSC.

In the present study, we conducted a large-scale GWAS for CSC followed by replication analyses using three independent Japanese and European cohorts. Our analysis using 1,546 CSC cases and 13,029 controls identified two novel CSC susceptible loci, rs13278062 at *TNFRSF10A-LOC389641* and rs6061548 near *GATA5*, which were significantly associated with the disease on a genome-wide scale. As these single-nucleotide polymorphisms (SNPs) showed a robust and homogenous effect among the Japanese and European cohorts, they may be important targets for further molecular biological evaluation and the development of new treatments.

Results

GWAS for CSC and replication analyses in Japanese cohorts

After stringent quality control, 2,893,743 SNPs were included in the first stage of the GWAS in a Japanese case-control cohort consisting of 610 CSC patients and 2,850 controls. We included three principal components as covariates to adjust for possible population stratification, which provided an acceptable control; the genomic inflation factor lambda (λ_{GC}) was 1.157. The quantile-quantile plot is shown in Supplementary Fig. 1.

To examine whether a population substructure existed and its influence on the GWAS results, we performed principal component analysis (PCA) for the current study using publicly available multiethnic genotype data from 1000 Genome project (Phase 3, ftp://ftp.1000genomes.ebi.ac.uk/vol1/ftp/release/20130502/) (Supplementary Fig. 2) and without this data (Supplementary Fig. 3). The analyses revealed that nearly all subjects in our discovery GWAS fell into the Japanese cluster, whereas a mild population substructure existed within the current discovery GWAS.

In the first stage, we identified two loci showing a suggestive *P*-value of $< 1.0\times10^{-6}$ for rs13278062 at *TNFRSF10A-LOC389641* ($OR_{discovery} = 1.38$, $P_{discovery} = 5.94 \times 10^{-7}$) and rs6061548 near *GATA5* ($OR_{discovery} = 1.61$, $P_{discovery} = 2.52 \times 10^{-7}$). The Manhattan plot, regional plots and linkage disequilibrium plots are shown in Figure 1, Figure 2 and Supplementary Fig. 4, respectively. Downstream of rs13278062, some SNPs in the *CHMP7* region showed relatively low *P* values.

No variants were observed downstream of rs6061548 in the regional plot probably owing to stringent QC. Therefore, we made a regional plot around rs6061548 using the GWAS results before QC was applied. In this regional plot, many SNPs within *GATA5* showed low *P*-values; the most significant association was found at rs13044490 within *GATA5* (OR =1.67, $P = 2.94 \times 10^{-10}$, Supplementary Fig. 5).

In the replication stage using 278 independent CSC samples from Japan, both rs13278062 at *TNFRSF10A-LOC389641* (OR = 1.35, $P = 8.97 \times 10^{-4}$) and rs6061548 near *GATA5* (OR = 1.39, $P = 1.28\times 10^{-2}$) showed significant associations with CSC (Table 1).

The associations of 2 SNPs with CSC were further evaluated in another Japanese CSC case-control dataset. Using the data from Kobe University Hospital, we found that rs6061548 near *GATA5* was also significantly associated with CSC in this dataset (OR = 2.29, $P = 3.26 \times 10^{-6}$). Rs13278062 showed a trend towards an association with the same direction of effect (OR = 1.19, $P = 0.189$, Table 1).

Replication in a European cohort and meta-analysis

We conducted trans-ethnic replication analyses to confirm the association. Association analysis using 521 cases and 3,577 controls of European descent revealed that rs13278062 and rs6061548 were significantly associated with CSC in the European cohort (Table 1). The odds ratios of the SNPs in the European cohort were similar to that observed in the Japanese cohort ($OR_{European} = 1.36$, $P_{European} = 1.47 \times 10^{-5}$ for rs13278062, and $OR_{European} = 1.60$, $P_{European} = 5.80 \times 10^{-4}$ for rs6061548). A meta-analysis of the Japanese and European cohorts also revealed strong association between CSC and rs13278062 at *TNFRSF10A-LOC389641* ($OR_{meta\text{-}all} = 1.35$, $P_{meta\text{-}all} = 1.26 \times 10^{-13}$) as well as rs6061548 near *GATA5* ($OR_{meta\text{-}all} = 1.63$, $P_{meta\text{-}all} = 5.36 \times 10^{-13}$). As shown in Figure 3, the effects of rs13278062 and rs6061548 on CSC occurrence were homogenous among the Japanese and European cohorts.

Association of previously reported SNPs with CSC

Previous GWAS of CSC reported two susceptibility loci, *CFH* rs1329428 and *SLC7A5* rs11865049.[30,31] In the current GWAS, *CFH* rs1329428 showed a significant association with CSC (OR = 1.17, $P = 0.015$). *SLC7A5* rs11865049 showed the same direction of effect as previously reported but did not reach a significant value (OR =1.15, $P = 0.24$). These results are summarized in Table 2.

Expression in human tissue

A search in a publicly available quantitative trait locus analysis (eQTL) database revealed that rs13278062 was significantly associated with *TNFRSF10A* expression (GTEx Portal. https://gtexportal.org/home/), but not with any other genes nor *CHMP7*. A multi-tissue eQTL plot revealed that the normalized effect size (NES) of rs13278062 on *TNFRSF10A* expression was strongest in the adrenal gland (NES = -0.973, $P = 4.5 \times 10^{-39}$; Supplementary Fig. 6). Although it was unclear whether rs6061548 near *GATA5* affects the expression or function of any genes in the database, rs13044490 within *GATA5*, which was a top-hit SNP in the regional plot, was significantly associated with *GATA5* expression. The effect of rs13044490 on *GATA5* expression was strongest in the esophageal muscularis (NES = 0.347, $P = 3.9 \times 10^{-8}$; Supplementary Fig. 7).

To confirm the expression of the genes in the human retina and choroid that play a significant role in CSC pathogenesis, we conducted database searching using the Eyeintegration database (https://eyeintegration.nei.nih.gov/, v1.01) and The Ocular Tissue Database (https://genome.uiowa.edu/otdb/), the only databases that includes gene expression data in human retina and choroid. The Eyeintegration database showed that the expression of both *TNFRSF10A* and *GATA5* in the adult human RPE/choroid (n = 48) was stronger than that in the adult human retina (n = 52) as summarized in Figure 4. These results were supported by The Ocular Tissue Database, which shows that the expression of *TNFRSF10A* in the adult human RPE/choroid was stronger than that in the adult human retina (PLIER normalized expression level = 18.90 vs 16.34) and that of *GATA5* in the adult human RPE/choroid was also stronger than that in the adult human retina (PLIER normalized expression level = 57.26 vs 48.30). The Eyeintegration database revealed that the expression of both *TNFRSF10A* and *GATA5* was also observed in other human tissues (Supplementary Note).

Pathway analysis

We performed pathway analysis using VEGAS2Pathway (https://vegas2.qimrberghofer.edu.au/). In total, 9,723 pathways were evaluated. The top 10 pathways are shown in Supplementary Table 1. The most significantly associated pathway was the ESCRT-III complex (M00412, $P = 2.60 \times 10^{-5}$). However, no pathways reached the genome-wide, pathway-based significant *P*-value of less than 1.0×10^{-5}.[30,35]

Discussion

In the current study, we identified two novel susceptible loci, rs13278062 at *TNFRSF10A-LOC389641* and rs6061548 near *GATA5* for a common pachychoroid disease, CSC, through a large GWAS followed by replication studies in three independent case-control datasets of Japanese and European origin. These SNPs showed robust and consistent association among all datasets. Interestingly, rs13278062 has been reported to be a susceptibility SNP for AMD. As the relationship between AMD and CSC has received increased attention, the current results have significant scientific implications that improve the understanding of the similarities and differences between AMD and CSC.

TNFRSF10A was first identified as an AMD susceptibility locus in a Japanese population.[36] Although this association has been confirmed in other ethnicities, the effect of *TNFRSF10A* on AMD in Caucasians was reported to be weaker than that in Asian population.[37–39] Recently, some researchers reported a subgroup within AMD that incorporates the characteristics of CSC, such as thick choroid and choroidal vascular hyperpermeability.[7,17,19] Although the precise rate of the subgroup among patients with AMD is currently unknown, the rate is estimated to be higher in Asians than in Caucasians.[22,40] Taken together with the current result, we speculate that eyes with CNV, which is traditionally diagnosed as AMD, include CNV

secondary to CSC, which may occur more frequently in Asians compared to that Caucasians. In support of this, the effect of *TNFRSF10A* on CSC occurrence (OR = 1.38) in the present study was higher than that of traditional AMD occurrence in a previous study (OR_{forAMD} = 1.25 in Asian, and OR_{forAMD} = 1.11 in European).[39] It is also possible that *TNFRSF10A* has pleiotropic effects on both AMD and CSC. The effects of *TNFRSF10A* on AMD should be further evaluated while stratifying the data for the presence of a pachychoroid background.

CNV accompanied by the characteristics of CSC was recently termed as pachychoroid neovasculopathy, as the thickened choroid is the most characteristic clinical feature of the condition. Gene expression evaluation in ocular tissue supports the importance of the RPE/choroid regarding the etiology of pachychoroid neovasculopathy and CSC, as *TNFRSF10A* is more strongly expressed in the RPE/choroid than in the retina. However, the exact role of *TNFRSF10A* in CSC occurrence or choroidal structure is unclear. Considering that the adrenergic hormones are established risk factors for CSC,[41,42] and that the eQTL showed that the genotype of rs13278062 at *TNFRSF10A* was strongly associated with its expression in the adrenal gland, *TNFRSF10A* may affect the risk of CSC by modulating hormone secretion from the adrenal glands.

We additionally identified that rs6061548 near *GATA5* was associated with CSC. *GATA5* is known to play an important role in vascular system development.[43–45] A recent study showed that *GATA5* is expressed in the microvascular endothelial cells and that its inactivation in mice results in vascular endothelial dysfunction.[46] Considering the stronger expression of *GATA5* in the RPE/choroid than in the retina, we speculate that *GATA5* may affects the susceptibility to CSC through vascular endothelial dysfunction in the choriocapillaris, which constitutes the inner vascular layers of the choroid, composed largely of fenestrated

capillaries. This hypothesis is compatible with previous reports showing that eyes with CSC had choriocapillary hypoperfusion,[47,48] and primary choroidal ischemia.[48] *GATA5* is also known to play an important role in stomach development and gastric diseases.[49–51] Interestingly, *GATA5* is reported to be upregulated by *H.pylori* infection,[52] which is one of the risk factors of CSC.[10,12–14] As described above, *GATA5* may also be an important target for the further understandings of CSC.

The current study has many strengths and limitations. The main strengths are its large sample size and that multiple replication studies were performed in different ethnic groups, which led to robust results. As CSC is thought to be a benign, self-limiting disease, its genetic background has not been clarified. However, the pathology of CSC has become an important issue in relation to AMD. This study is the largest genetic study on CSC, and the first study to identify transethnically-robust susceptible genes using a non-hypothesis-driven, exploratory approach. Considering the identification of relatively high, consistent effects across multiple ethnic groups, the current study has strong scientific implications. However, the sample size of this study was still limited. An even larger sample size is required to identify additional susceptibility SNPs with low allele frequency or low effect size and to further elucidate disease pathways in CSC. Another limitation is the inflated λ_{GC} in our discovery GWAS, which may have led to false-positive associations. This inflation may be related to the presence of a mild population substructure, as inflation was still observed even after conducting the GWAS using samples genotyped with a single DNA microarray platform, OmniExpress (λ_{GC} = 1.098). However, the positive associations of both *TNFRSF10A-LOC389641* rs13278062 and near *GATA5* rs6061548 were still significant even after genomic control correction ($P_{meta} = 2.57 \times 10^{-12}$ and $P_{meta} = 6.29 \times 10^{-12}$, respectively; Supplementary Table 2), and thus these associations appear to be robust.

In summary, we identified two novel CSC susceptibility loci, rs13278062 at *TNFRSF10A-LOC389641* and rs6061548 near *GATA5,* using a total of 1,546 CSC cases and 13,029 controls. These variants showed robust, consistent, and mild to moderate associations with CSC across ethnicities. We confirmed that both genes are expressed in the choroid, which is the main focus of CSC and AMD. Our findings improve the understanding of the pathogenesis of CSC and AMD.

Methods

Patient enrolment

In the discovery GWAS, 610 Japanese patients with CSC were recruited from the Kyoto University Hospital, and 2,850 healthy Japanese controls were recruited from the Aichi Cancer Center Research Institute, Hayashi Eye Hospital, Mizoguchi Eye Hospital, Oita University Faculty of Medicine, Ideta Eye Hospital, Shinjo Eye Clinic, Miyata Eye Hospital, Ozaki Eye Hospital, Kyoto University Hospital, and Nagahama City Hospital. Detailed information of the control cohort is described elsewhere,[53] and is briefly summarized in the Supplementary Note and Supplementary Table 3.

In the first replication stage, 278 CSC patients were recruited from across Japan, particularly Kyoto University Hospital (N = 57), Kagawa University Hospital (N = 104), Yamanashi University Hospital (N = 80), and Fukushima Medical University Hospital (N = 37). Control allele frequency data were extracted from the genome-wide dataset of healthy Japanese subjects from the Tohoku Medical Megabank Organization (N = 3,498),[54–56] Kyoto University (N = 3,074),[57,58] and Yokohama City University dataset (N = 1,048). Detailed information is shown in the Supplemental Note. In the second and the third replication stages,

the Kobe CSC case-control dataset, which consists of 137 Japanese patients with CSC and 1,153 Japanese controls, and European CSC case-control dataset, which consists of 521 European patients with CSC and 3,577 European controls, were utilized, respectively. Although the detailed information for this dataset has been described previously, [30,31] a brief summary is also provided in the Supplemental Note.

All procedures adhered to the tenets of the Declaration of Helsinki. The Institutional Review Board and Ethics Committee of each participating institute approved the respective study protocols. All patients were fully informed of the purpose and procedures of the study, and written consent was obtained from all patients prior to their participation in the study.

Diagnosis of patients with CSC

All patients underwent a comprehensive ophthalmic examination, including visual acuity measurement; slit-lamp biomicroscopy; dilated fundoscopy; color fundus photography; and optical coherence tomography (OCT) examination including enhanced depth imaging, fundus autofluorescence, fluorescein angiography, and indocyanine green angiography CSC was diagnosed based on medical history, serous retinal detachment, thickened choroid with dilated choroidal vessels seen on OCT, choroidal vascular hyperpermeability on ndocyanine green angiography, and/or leakages on fluorescein angiography at the level of the RPE. Based on these findings, two retina specialists (M.M. and Y.H.) diagnosed the patients independently, and discrepancies were adjusted in a face-to-face consensus session. Patients with other causes of fluorescein leakage or serous retinal detachment unrelated to CSC (e.g., AMD, intraocular inflammation, diabetic retinopathy, or retinal vein occlusion) were excluded from the study. In the second and third replication stages, patients with CSC were

diagnosed based on previously described criteria.[29–31] The details are summarized in the Supplementary Note.

Genotyping

Genomic DNA was extracted from peripheral blood samples according to standard laboratory procedures. A series of BeadChip DNA arrays (Illumina, San Diego, CA, USA), namely Omni Express (N = 250) and Asian Screening Array (N = 360), were used for genotyping the CSC samples, while Human610-Quad BeatChip (N = 1,194) and Omni Express (N = 1,656) were used for genotyping the control samples.

Genotype imputation was performed using the Michigan imputation server (https://imputationserver.sph.umich.edu/index.html#!pages/home) with the 1000 Genome dataset (phase3 v5 release) of East Asians as a reference panel for each dataset. In each dataset, SNPs with a call rate <90% or a minor allele frequency <1% were excluded before genotype imputation. Imputed SNPs for which R^2 was less than 0.9 were excluded from the subsequent association analysis. Next, SNPs with a call rate <90%, a minor allele frequency <1%, or significant deviation ($P < 1.0 \times 10^{-5}$) from Hardy-Weinberg equilibrium were excluded from further statistical analysis, and samples with a call rate <90 % were also excluded. We checked the allelic discrimination of SNPs showing a suggestive association with CSC in the discovery GWAS ($P < 1.0 \times 10^{-5}$) for each platform. We excluded SNPs with an insufficient quality of allelic discrimination and their proxy SNPs ($R^2 > 0.8$). Finally, 2,893,743 SNPs from 610 CSC samples and 2,850 control samples were used for discovery stage analysis.

In the first replication stage, genotypes of CSC samples (N = 278) were determined using a commercially available assay (TaqMan SNP assay with the ABI PRISM 7700 system; Applied Biosystems, Foster City, CA, USA). We extracted the allele frequency from existing healthy Japanese genome-wide datasets, which included the Tohoku dataset,[54–56] Kyoto University,[57,58] and Yokohama City University datasets. The details of the genotyping methods are summarized in the Supplementary Note. Briefly, the Integrative Japanese Genome Variation Database (ver 3.5K JPN, https://ijgvd.megabank.tohoku.ac.jp/) provides genomic reference panels obtained from 3,554 normal Japanese subjects recruited from the Tohoku Medical Megabank Organization, Iwate Medical Megabank Organization, Nagahama Prospective Cohort for Comprehensive Human Bioscience, and National Hospital Organization Nagasaki Medical Center. All DNA samples were whole genome-sequenced using the Illumina HiSeq 2500. The Human Genetic Variation Database is a database of genomic reference panels released from Kyoto University (http://www.hgvd.genome.med.kyoto-u.ac.jp/index.html). This database is a web-accessible resource of genetic variations in the Japanese population. Whole-genome SNV genotyping was performed for 3,712 individuals, who formed a subset of participants of The Nagahama Prospective Genome Cohort for the Comprehensive Human Bioscience (the Nagahama Study), with the Illumina HumanHap610 quad, Omni 2.5M and Human exome Beadarrays (Illumina). The Yokohama City University dataset includes 1,048 Japanese healthy controls recruited from the Yokohama City University, Okada Eye Clinic, and Aoto Eye Clinic in Yokohama, Kanagawa Prefecture, Japan. Genotypes of samples from Yokohama City University were determined using BeadChip DNA arrays, namely Human OmniExpress chip (Illumina), with the standard protocol recommended by each manufacturer.

The Kobe CSC case-control dataset, which was used in the second replication stage, was genotyped using the Human Omni Express BeadChips (Illumina, San Diego, CA, USA) as described elsewhere.[31] Genomic imputation was performed for the dataset using the BEAGLE 4.1 and 1000 genomes dataset (phase3 v5 release) as the reference panels. Imputed SNPs for which $R^2 < 0.7$ were excluded from the imputed dataset. The association of SNPs with CSC was tested by logistic regression analysis with no adjustment. The European CSC case-control dataset, which was used in the third replication stage, was genotyped using OmniExpress-12 or OmniExpress-24chip. The data were imputed with the Haplotype Reference Consortium release 1.1.2016, and were stringent quality controls were performed as described previously.[30]

Statistical analyses

Genome-wide logistic regression analysis was conducted for the CSC, adjusting for three principal components. Because information on age and sex was not available for 1,656 out of the 2,850 control samples, adjustment for these factors was not performed in the discovery GWAS. Experiment-wide significance in the discovery stage was set to $P = 5.0 \times 10^{-8}$. We carried SNPs with *P*-value of less than 1.0×10^{-6} forward to the replication stage. In the first and second replication stages, logistic regression was performed for the SNPs that showed suggestive association in the first stage. All meta-analyses were performed using the fixed effect model. Thereafter, differences were considered significant at $P < 0.05$. Deviations in genotype distributions from Hardy-Weinberg equilibrium were assessed with chi-square tests. These statistical analyses were performed with R ver 3.5.2 (R Foundation for Statistical Computing, Vienna, Austria; available at http://www. rproject.org/), GCTA ver. 1.25.3 (http://cnsgenomics.com/software/gcta/index.html#Overview) and PLINK ver. 2.0 (https://www.cog-genomics.org/plink/2.0/).

In the third replication stage using the European dataset, association analysis was performed using the Firth bias-corrected likelihood ratio test, implemented in EPACTS (version 3.2.6, https://genome.sph.umich.edu/wiki/EPACTS; University of Michigan), correcting for sex and the first two components of ancestry analysis.

Pathway analysis

Using the GWAS summary statistics and *P* values of replicated SNPs, we performed gene-based analysis and clustered genes into pathways using VEGAS2pathway (https://vegas2.qimrberghofer.edu.au/, version 2). Briefly, VEGAS2 successively prunes the list of variants with r^2 criteria of 0.99, 0.90, 0.70 and 0.50, if a gene contains more than 1000 SNPs. After each pruning interval, VEGAS2 checks the number of pruned SNPs. If the number of pruned SNPs is less than 1000, VEGAS2 uses the pruned SNPs from that interval to perform gene-based analysis; otherwise, it iteratively applies an increasingly stringent r^2 criteria on all SNPs in the gene. After applying a pruning criterion of $r^2 = 0.50$, it uses all pruned SNPs for analysis irrespective of the number. The gene list was obtained from the VEGAS2 official site (https://vegas2.qimrberghofer.edu.au/glist-hg19). Obtained gene-based result was used to perform calculate pathway-based tests and empirical *P*-values to obtain the significance of each pathway. Regions +/- 0kb outside of genes were defined as gene regions, and all SNPs were used for analysis. For the SNPs that were carried forward for to the replication stage, *P* values from meta-analysis were used rather than GWAS *P* values. The Biosystems gene-pathway annotation file was obtained from the VEGAS2 official site (https://vegas2.qimrberghofer.edu.au/biosystems20160324.vegas2pathSYM). The significance threshold of the empirical *P* value in the pathway analysis was set to 1.0×10^{-5}.[30,35]

Database search

To determine the existence of a population substructure and its influence on the GWAS results, publicly available genotype data from five populations, including African, South Asian, European, East Asian, and Japanese (1000 Genome project, Phase 3, ftp://ftp.1000genomes.ebi.ac.uk/vol1/ftp/release/20130502/) were used for PCA

Searching of the publicly available quantitative trait locus analysis (eQTL) database (Genotype-Tissue Expression (GTEx) Portal: https://gtexportal.org/home/) revealed an association between the SNP genotypes and gene expression in multiple human tissues. NES is defined as the slope of the linear regression and is computed as the effect of the alternative allele relative to the reference allele.

Expression of genes in the adult human retina and RPE was explored in the eyeintegration database (https://eyeintegration.nei.nih.gov/, v1.01. accessed 10 April 2019). The database lists the expression levels of genes given in transcripts per million. Gene expression levels were compared by Wilcoxon test. Expression of genes in the human retina and choroid was explored in The OCULAR TISSUE DATABASE (https://genome.uiowa.edu/otdb/, accessed 28 February 2019). This database provides quantitative expression level of genes in ocular tissues determined by the PLIER (Probe Logarithmic Intensity Error) algorithm.

Data Availability

Top SNPs (n = 100) in the discovery GWAS can be available as Supplementary Data 1. The source data about the expression of genes in the adult human retina and RPE can be available as Supplementary Data 2. The complete GWAS summary data can be visualised here:

https://figshare.com/articles/CSC_control_PC3_assoc_logistic/11136047. The datasets generated during the current study are also available from the corresponding author on reasonable request.

Acknowledgments

We thank Ms. Hatsue Hamanaka for assistance with genotyping. We thank for Dr. Masato Akiyama for supervising about method of the pathway analysis.

Author contributions

Y.H., M.M., R.Y., F.M., K.Y., and A.T. designed the study; Y.H., M.M., R.L.S., C.J.F.B., C.B.H., A.M., A.M., Y.S., Y.S., Y.T., M.H., Y.M., H.N., A.O., S.O., H.T., A.U., M.M., A.T., N.U.A, A.T., T.S., N.M., C.S., T.I., S.H., E.K.D.J., A.I.D.H., K.Y., and A.T. performed the study; Y.H., M.M., R.L.S., C.J.F.B., C.B.H., A.M., A.M., A.T., T.S., N.M., C.C.K., T.Y.W., R.Y., S.H., E.K.D.J., A.I.D.H., K.Y., and A.T. analyzed the data; and Y.H., M.M., and K.Y. prepared the manuscript.

Competing interests

The Authors declare no Competing Financial or Non-Financial Interests

References

1. Gemenetzi, M., De Salvo, G. & Lotery, A. J. Central serous chorioretinopathy: an update on pathogenesis and treatment. *Eye* **24,** 1743-1756 (2010).

2. Kitzmann, A. S., Pulido, J. S., Diehl, N. N., Hodge, D. O. & Burke, J. P. The incidence of central serous chorioretinopathy in Olmsted county, Minnesota, 1980-2002. *Ophthalmology* **115,** 169-173 (2008).

3. Nicholson, B., Noble, J., Forooghian, F. & Meyerle, C. Central serous chorioretinopathy: update on pathophysiology and treatment. *Surv. Ophthalmol.* **58,** 103-126 (2013).

4. Bujarborua, D. Long-term follow-up of idiopathic central serous chorioretinopathy without laser. *Acta Ophthalmol. Scand.* **79,** 417-421 (2001).

5. Breukink, MB. et al. Chronic central serous chorioretinopathy: long-term follow-up and vision-related quality of life. *Clin Ophthalmol*. **11**, 39-46 (2016).

6. Mrejen, S. *et al.* Long-term visual outcomes and causes of vision loss in chronic central serous chorioretinopathy. *Ophthalmology* (2019). doi:10.1016/j.ophtha.2018.12.048

7. Shiragami, C. *et al.* Clinical features of central serous chorioretinopathy with Type 1 choroidal neovascularization. *Am. J. Ophthalmol.* **193,** 80-86 (2018).

8. Daruich, A. *et al.* Central serous chorioretinopathy: Recent findings and new

physiopathology hypothesis. *Prog. Retin. Eye Res.* **48,** 82-118 (2015).

9. Yannuzzi, L. Type-A behavior and central serous chorioretinopathy. *Retina* **7:2,** 111-131 (1987).

10. Haimovici, R., Koh, S., Gagnon, D. R., Lehrfeld, T. & Wellik, S. Risk factors for central serous chorioretinopathy: a case-control study. *Ophthalmology* **111,** 244-249 (2004).

11. Weenink, A. A. C., Borsje, R. A. & Oosterhuis, J. A. J. A. Familial chronic central serous chorioretinopathy. *Ophthalmologica* **215,** 183-187 (2001).

12. Mateo-Montoya, A. & Mauget-Faÿse, M. Helicobacter pylori as a risk factor for central serous chorioretinopathy: literature review. *World J. Gastrointest. Pathophysiol.* **5,** 355-358 (2014).

13. Bagheri, M., Rashe, Z., Ahoor, M. H. & Somi, M. H. Prevalence of Helicobacter pylori infection in patients with central serous chorioretinopathy: a review. *Med. hypothesis, Discov. Innov. Ophthalmol. J.* **6,** 118-124 (2017).

14. Zavoloka, O. Helicobacter pylori is the culprit behind central serous chorioretinopathy. *Graefe's Arch. Clin. Exp. Ophthalmol.* **254,** 2071 (2016).

15. Wang, M. *et al.* Central serous chorioretinopathy. *Acta Ophthalmol.* **86,** 126–145 (2008).

16. Spaide, R. F. *et al.* Central serous chorioretinopathy in younger and older adults.

Ophthalmology **103,** 2070–2080 (1996).

17 Pang, C. E. & Freund, K. B. Pachychoroid neovasculopathy. *Retina* **35,** 1-9 (2015).

18. Lehmann, M., Bousquet, E., Beydoun, T. & Behar-Cohen, F. Pachychoroid: An inherited condition? *Retina* **35,** 10-16 (2015).

19. Miyake, M. *et al.* Pachychoroid neovasculopathy and age-related macular degeneration. *Sci. Rep.* **5,** 16204 (2015).

20. Fung, A. T., Yannuzzi, L. A. & Bailey Freund, K. Type 1 (Sub-retinal pigment epithelial) neovascularization in central serous chorioretinopathy masquerading as neovascular age-related macular degeneration. *Retina* **32,** 1829-1837 (2012).

21. Azar, G. *et al.* Pachychoroid neovasculopathy: aspect on optical coherence tomography angiography. *Acta Ophthalmol.* **95,** 421-427 (2017).

22. Cheung, C. M. G. *et al.* Pachychoroid disease. *Eye* **33**, 14-33 (2019).

23. Gallego-Pinazo, R., Dolz-Marco, R. & Freund, K. B. in *Choroidal Disorders* 161-170 (Academic Press, 2017). doi:10.1016/B978-0-12-805313-3.00010-7

24. Hata, M. *et al.* Intraocular vascular endothelial growth factor levels in pachychoroid neovasculopathy and neovascular age- related macular degeneration. *Investig. Ophthalmol. Vis. Sci.* **58,** 292-298 (2017).

25. Akkaya, S. Spectrum of pachychoroid diseases. *Int. Ophthalmol.* 1–8 (2017). doi:10.1007/s10792-017-0666-4

509 26. Klein, R. J., Robert, J., Emily, Y. & Tsai, J. Complement factor H polymorphism in
510 age-related macular degeneration. *Science (80-.).* **308,** 385-389 (2005).
511 27. Miki, A. *et al.* Common variants in the complement factor H gene confer genetic
512 susceptibility to central serous chorioretinopathy. *Ophthalmology* **121,** 1067-1072
513 (2014).
514 28. Hosoda, Y. *et al.* CFH and VIPR2 as susceptibility loci in choroidal thickness and
515 pachychoroid disease central serous chorioretinopathy. *Proc. Natl. Acad. Sci. U. S. A.*
516 **115,** 6261-6266 (2018).
517 29. De Jong, E. K. *et al.* Chronic central serous chorioretinopathy is associated with
518 genetic variants implicated in age-related macular degeneration. *Ophthalmology* **122,**
519 562-570 (2015).
520 30. Schellevis, R. L. *et al.* Role of the complement system in chronic central serous
521 chorioretinopathy: A genome-wide association study. *JAMA Ophthalmol.* (2018).
522 doi:10.1001/jamaophthalmol.2018.3190
523 31. Miki, A. *et al.* Genome-wide association study to identify a new susceptibility locus
524 for central serous chorioretinopathy in the Japanese population. *Investig.*
525 *Opthalmology Vis. Sci.* **59,** 5542 (2018).
526 32. Dijk, E. van *et al.* Association of a haplotype in the NR3C2 gene, encoding the
527 mineralocorticoid receptor, with chronic central serous chorioretinopathy.

Ophthalmology **135,** 446-451 (2017).

33. Mohabati, D. *et al.* Genetic risk factors in acute central serous chorioretinopathy. *Retina* 1 (2018). doi:10.1097/IAE.0000000000002333

34. Breukink, M. B. *et al.* Genomic copy number variations of the complement component C4B Ggene are associated with chronic central serous chorioretinopathy. *Invest. Ophthalmol. Vis. Sci.* **56,** 5608-5613 (2015).

35. Mishra, A. & MacGregor, S. A novel approach for pathway analysis of GWAS data highlights role of BMP signaling and muscle cell differentiation in colorectal cancer susceptibility. *Twin Res. Hum. Genet.* **20,** 1-9 (2017).

36. Arakawa, S. *et al.* Genome-wide association study identifies two susceptibility loci for exudative age-related macular degeneration in the Japanese population. *Nat. Genet.* **43,** 1001-1005 (2011).

37. Fritsche, L. G. *et al.* Seven new loci associated with age-related macular degeneration. *Nat. Genet.* **45,** 433-439 (2013).

38. Sun, Y. *et al.* TNFRSF10A-LOC389641 rs13278062 but not REST-C4orf14-POLR2B-IGFBP7 rs1713985 was found associated with age-related macular degeneration in a Chinese population. *Invest. Ophthalmol. Vis. Sci.* **54,** 8199-8203 (2013).

39. Fritsche, L. G. *et al.* A large genome-wide association study of age-related macular

degeneration highlights contributions of rare and common variants. *Nat. Genet.* **48,** 134-143 (2016).

40. Cheung, C. M. G. *et al.* Association between choroidal thickness and drusen subtypes in age-related macular degeneration. *Ophthalmol. Retin.* **2,** 1196–1205 (2018).

41. Gass, J. D. M. & Little, H. Bilateral bullous exudative retinal detachment complicating idiopathic central serous chorioretinopathy during systemic corticosteroid therapy. *Ophthalmology* **102,** 737-747 (1995).

42. Bouzas, E. A., Karadimas, P. & Pournaras, C. J. Central serous chorioretinopathy and glucocorticoids. *Survey of Ophthalmology* **47,** 431–448 (2002).

43. Jiang, J.-Q. *et al.* Prevalence and spectrum of GATA5 mutations associated with congenital heart disease. *Int. J. Cardiol.* **165,** 570-573 (2013).

44. Stennard, F. A. *et al.* Cardiac T-box factor Tbx20 directly interacts with Nkx2-5, GATA4, and GATA5 in regulation of gene expression in the developing heart. *Dev. Biol.* **262,** 206-224 (2003).

45. Reiter, J. F. *et al.* Gata5 is required for the development of the heart and endoderm in zebrafish. *Genes Dev.* **13,** 2983-2995 (1999).

46. Messaoudi, S. *et al.* Endothelial Gata5 transcription factor regulates blood pressure. *Nat. Commun.* **6,** 8835 (2015).

47. Cakir, B. *et al.* OCT Angiography of the choriocapillaris in central serous

566 chorioretinopathy: a quantitative subgroup analysis. *Ophthalmol. Ther.* (2019).
567 doi:10.1007/s40123-018-0159-1
568 48. Rochepeau, C. *et al.* Optical coherence tomography angiography quantitative
569 assessment of choriocapillaris blood flow in central serous chorioretinopathy. *Am. J.*
570 *Ophthalmol.* **194,** 26-34 (2018).
571 49. Wang, X. et al. Epigenetic subgroups of esophageal and gastric adenocarcinoma with
572 differential GATA5 DNA methylation associated with clinical and lifestyle factors.
573 *PLoS One*. (2011). doi:10.1371/journal.pone.0025985.
574 50. Sobota, RS. et al. Epigenetic and genetic variation in GATA5 is associated with gastric
575 disease risk. *Hum Genet*. **8**, 895-906 (2016).
576 51. Fukuda, K, Yasugi, S. The molecular mechanisms of stomach development in
577 vertebrates. *Dev Growth Differ*. **6**, 375-382 (2005).
578 52. Wen, X. Z. *et al.* Methylation of GATA-4 and GATA-5 and development of sporadic
579 gastric carcinomas. *World J. Gastroenterol.* **16,** 1201-1208 (2010).
580 53. Aung, T. *et al.* A common variant mapping to CACNA1A is associated with
581 susceptibility to exfoliation syndrome. *Nat. Genet.* 2015 Apr;47 (4): 387-92.
582 54. Kuriyama, S. *et al.* The Tohoku medical megabank project: Design and mission. *J.*
583 *Epidemiol.* **26,** 493-511 (2016).
584 55. Yamaguchi-Kabata, Y. *et al.* iJGVD: an integrative Japanese genome variation

database based on whole-genome sequencing. *Hum. Genome Var.* **2,** 15050 (2015).

56. Nagasaki, M. *et al.* Rare variant discovery by deep whole-genome sequencing of 1,070 Japanese individuals. *Nat. Commun.* **6,** 8018 (2015).

57. Narahara, M. *et al.* Large-scale East-Asian eQTL mapping reveals novel candidate genes for LD mapping and the genomic landscape of transcriptional effects of sequence variants. *PLoS One* **9,** e100924 (2014).

58. Higasa, K. *et al.* Human genetic variation database, a reference database of genetic variations in the Japanese population. *J. Hum. Genet.* **61,** 547-553 (2016).

Figure legends

Figure 1. Manhattan plot for discovery GWAS using 610 patients with central serous chorioretinopathy and 2,580 control participants.

Each plot shows −log10-transformed *P*-values for all SNPs. The horizontal solid line represents the genome-wide significance threshold of $P = 5.0 \times 10^{-8}$, and the lower broken line represents the suggestive threshold of $P = 1.0 \times 10^{-6}$. Two SNPs exceeded the suggestive threshold; rs13278062 at *TNFRSF10A-LOC389641* ($P = 5.94 \times 10^{-7}$) and rs6061548 near *GATA5* ($P = 2.52 \times 10^{-7}$).

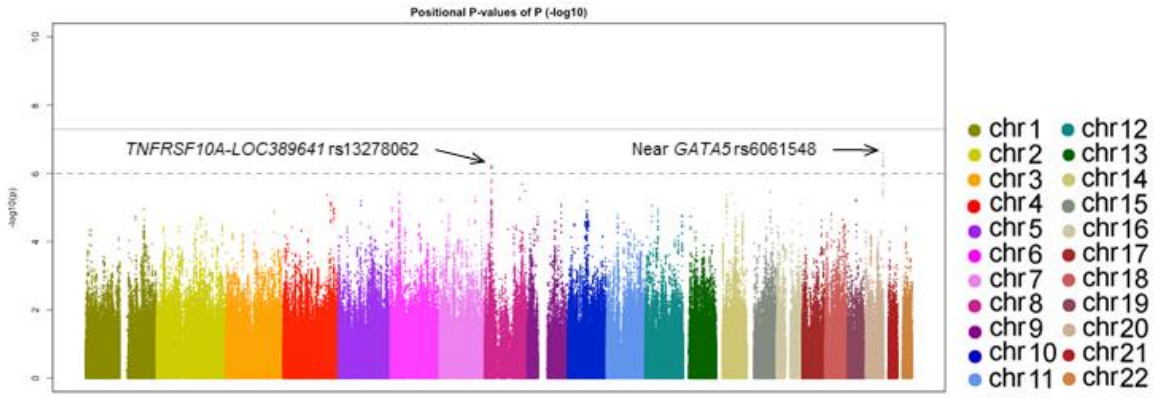

Figure 2. Regional association plots of evaluated SNPs around two suggestive SNPs in discovery GWAS. Plots represent the −log10 (*P*-values) obtained from the first-stage GWAS. Each plot corresponds to the following; (A) *TNFRSF10A-LOC389641* and (B) near *GATA5* regions.

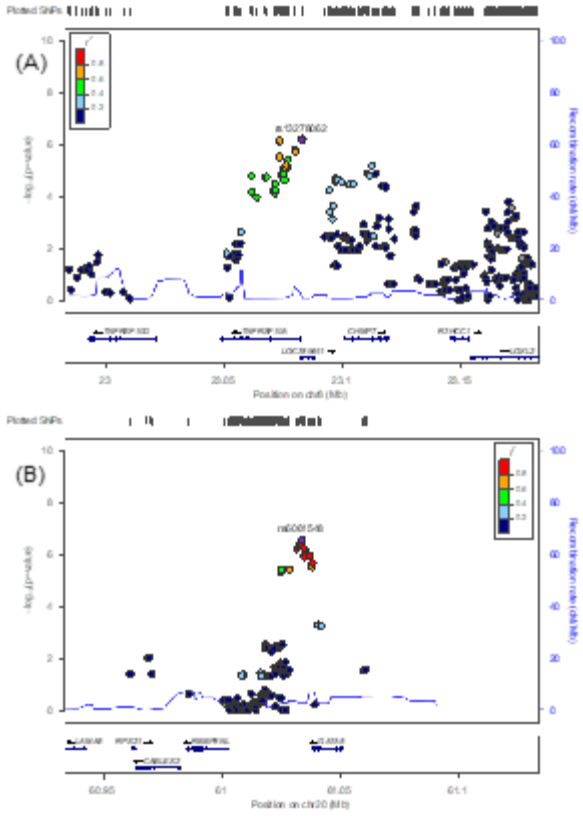

Figure 3: Forest plots showing the effects of (A) rs13278062 and (B) rs6061548 on CSC in each cohort and meta-analysis

Both SNPs showed robust, consistent, and mild to moderate association with CSC across ethnic groups.

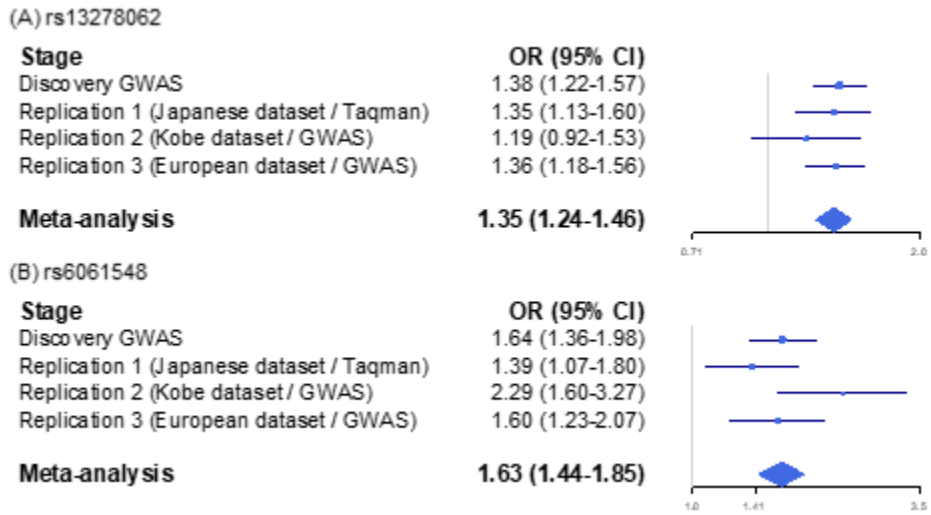

Figure 4. Boxplots of *TNFRSF10A* and *GATA5* expression levels in the human retina and RPE/choroid.

Expression levels of *TNFRSF10A* and *GATA5* in the human retina (n = 52) and RPE/choroid (n = 48) are given in transcripts per million (TPM). *TNFRSF10A* was strongly expressed in the human RPE/choroid compared to in the retina (116.62 ± 58.53 vs 18.11 ± 8.96 TPM, $P < 0.001$). *GATA5* was also strongly expressed in the human RPE/choroid compared to in the retina (69.05 ± 37.91 vs 4.66 ± 7.08 TPM, $P < 0.001$). TPM values are expressed as the mean ± standard deviation and compared by Wilcoxon test.

RPE; retinal pigment epithelium

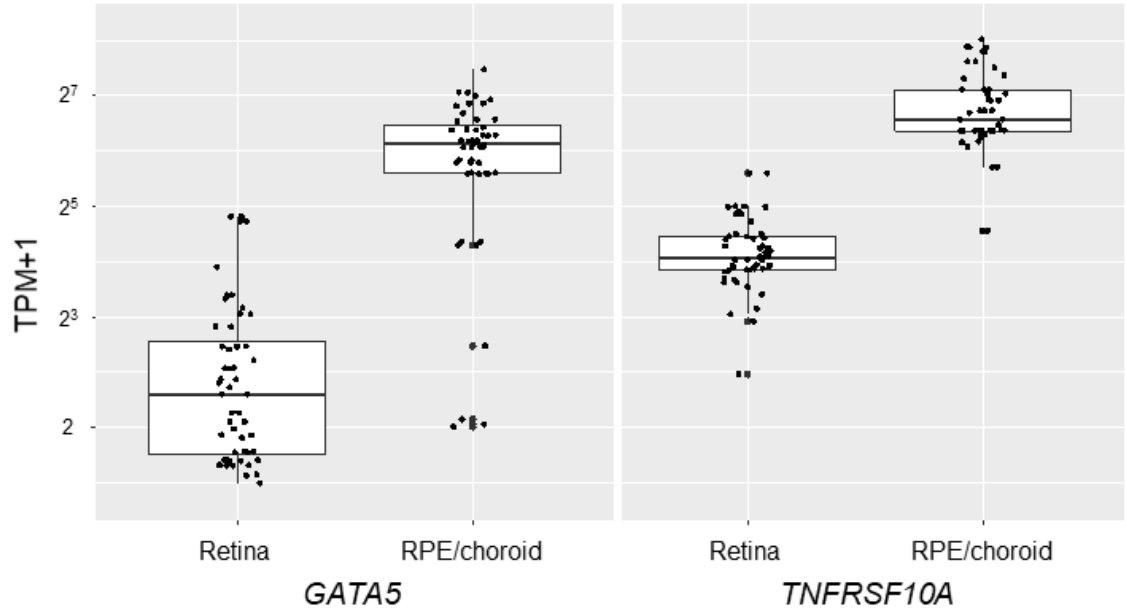

Table 1. Discovery and replication analyses to identify SNPs associated with CSC.

CHR: chromosome, EAF: effect allele frequency, CSC: central serous chorioretinopathy, OR: odds ratio, CI: confidence interval. All meta-analyses were performed using a fixed-effect model.

**P*-values were derived using logistic regression analysis. †*P*-values were derived using association analysis.

	SNP	rs13278062						rs6061548					
	Nearby genes	*TNFRSF10A-LOC389641* (in gene)						*GATA5* (Nearby)					
	Effect Allele	T						T					
	CHR: position	8: 23082971						20: 61033892					
Stage	Ethnicities	CSC		Control		OR (95% CI)	P	CSC		Control		OR (95% CI)	P
		N	EAF	N	EAF			N	EAF	N	EAF		
Discovery GWAS	Japanese	610	0.421	2,850	0.345	1.38 (1.22–1.57)	5.94×10^{-7}*	610	0.138	2,850	0.088	1.64 (1.36–1.98)	2.52×10^{-7}*
Replication stage 1	Japanese	277	0.392	5,449	0.324	1.35 (1.13–1.60)	8.97×10^{-4}*	278	0.128	4,546	0.095	1.39 (1.07–1.80)	0.0128*
Replication stage 2	Japanese	137	0.409	1,153	0.368	1.19 (0.92–1.53)	0.189*	137	0.161	1,153	0.077	2.29 (1.60–3.27)	5.55×10^{-6}*
Replication stage 3	European	521	0.591	3,577	0.520	1.36 (1.18–1.56)	1.47×10^{-5}†	521	0.082	3,577	0.051	1.60 (1.23–2.07)	5.80×10^{-4}†
Meta-analysis of Japanese Data (Discovery + Replication 1 + Replication 2)													
	Japanese	1,024		9,452		1.34 (1.22–1.48)	1.45×10^{-9}	1,025		8,549		1.64 (1.43–1.89)	3.38×10^{-12}
Meta-analysis of Japanese Data and European Data													
	Japanese and European	1,545		13,029		1.35 (1.24–1.46)	1.26×10^{-13}	1,546		12,126		1.63 (1.44–1.85)	5.36×10^{-15}

Table 2. Association of previously reported SNPs on GWAS study with CSC

CHR: chromosome, EAF: effect allele frequency in the discovery stage, CSC: central serous chorioretinopathy, OR: odds ratio, CI: confidence interval.

**P*-values were derived using logistic regression analysis.

SNP	Gene	CHR	Position	Effect allele	EAF in CSC (N = 610)	EAF in control (N = 2,850)	OR (95% CI)	*P**	Effect directions as reported
rs1329428	*CFH*	1	196702810	T	0.506	0.466	1.17 (1.03–1.32)	1.45×10^{-2}	+
rs11865049	*SLC7A5*	16	87874140	A	0.078	0.069	1.15 (0.91–1.44)	0.24	+

Supplementary Information

Supplementary Note

Description of the cohorts and genotyping

Discovery GWAS

CSC patients (n = 610) were recruited from Kyoto University Hospital. The diagnosis was made as described in the Methods section. For controls, existing genome-wide datasets were utilized. The data for the healthy Japanese cohort (n = 2,850) were drawn from eight institutions across Japan (Aichi Cancer Center Research Institute, Hayashi Eye Hospital in Fukuoka, Mizoguchi Eye Hospital in Nagasaki, Department of Ophthalmology, Oita University Faculty of Medicine, and four sites in Miyazaki: Ideta Eye Hospital, Shinjo Eye Clinic, Miyata Eye Hospital, and Ozaki Eye Hospital, Kyoto University Hospital, and Nagahama City Hospital). Although detailed ophthalmic examinations were not performed for healthy Japanese subjects from the Aichi Cancer Center Research Institute (n = 1,194), the other 1,656 samples were confirmed to not have exfoliation syndrome, macular degeneration, or glaucoma, as described previously.[1] A series of BeadChip DNA arrays (Illumina, San Diego, CA, USA), namely Omni Express (n = 250) and Asian Screening Array (n = 360) were used for genotyping the CSC patients, and Human610-Quad BeatChip (n = 1,194) and Omni Express (n = 1,656) were used for genotyping of the control samples. SNPs with a call

rate <90% or minor allele frequency (MAF) <1% were excluded, and genotype imputation was performed using the Michigan imputation server (https://imputationserver.sph.umich.edu/index.html#!pages/home) with the 1000 Genomes dataset (phase3 v5 release) of East Asian subjects as a reference panel, and Eagle v2.3 was used as phasing software. Quality control was again performed for each platform after imputation; SNPs with a call rate <90%, MAF <1%, significant deviation ($P < 1.0 \times 10^{-5}$) from Hardy–Weinberg equilibrium, or call rate <90% were excluded from further analyses. We evaluated the allelic discrimination of SNPs showing a suggestive association with CSC in the discovery GWAS ($P < 1.0 \times 10^{-5}$) for each platform. We excluded SNPs with an insufficient quality of allelic discrimination and their proxy SNPs ($R^2 > 0.8$). Finally, 2,893,743 SNPs from 610 CSC samples and 2,850 control samples were used for discovery stage analysis.

Replication Stage 1

CSC cohort

For the replication stage, additional patients with CSC (n = 278) were recruited from across Japan (Kyoto University Hospital, Kagawa University Hospital, Yamanashi University Hospital, and the Fukushima Medical University Hospital). The diagnosis was made by ophthalmologists at each institute based on dilated fundus examination, optical coherence

tomography, and/or fluorescein and indocyanine green angiography. Genotypes were determined using a commercially available TaqMan SNP assay (Applied Biosystems, Foster City, CA, USA). Deviation from Hardy-Weinberg Equilibrium was assessed using R software.

Integrative Japanese Variation Database (Tohoku Dataset)

The Integrative Japanese Genome Variation Database (ver 3.5K JPN, https://ijgvd.megabank.tohoku.ac.jp/) provides genomic reference panels obtained from 3,554 normal Japanese subjects. Details of this cohort are described elsewhere.[2–4] Briefly, samples were recruited from the Tohoku Medical Megabank Organization, Iwate Medical Megabank Organization, Nagahama Prospective Cohort for Comprehensive Human Bioscience, and National Hospital Organization Nagasaki Medical Center. All DNA samples were whole genome-sequenced using the Illumina HiSeq 2500. This dataset contains the allele frequency data for 37,067,715 reliable autosomal single-nucleotide variations (SNVs) detected by whole-genome sequencing of 3,552 Japanese individuals (3.5KJPN release September 28, 2017). We used the dataset of 7,931,579 SNVs with more than or equal to 1% of the Japanese population allele frequency. Genotypes of rs13278062 and rs6061548 were available.

Human Genetic Variation Database (Kyoto University)

The Human Genetic Variation Database is a database of genomic reference panels released from Kyoto University (http://www.hgvd.genome.med.kyoto-u.ac.jp/index.html). The details of this database are described elsewhere.[5,6] Briefly, this database is a web-accessible resource of genetic variations in the Japanese population and contains 1,794,196 variants of 3,248 healthy individuals and 287,588 SNVs additionally identified by whole-exome sequencing of 1,208 healthy individuals. Whole-genome SNV genotyping was performed for 3,712 individuals, who formed a subset of participants of The Nagahama Prospective Genome Cohort for the Comprehensive Human Bioscience (the Nagahama Study), with the Illumina HumanHap610 quad, Omni 2.5M and Human exome Beadarrays (Illumina). After excluding samples for which the genotyping call rates were lower than 95%, kinship analysis and principal component analysis were applied. A total of 302 related individuals were excluded from further analysis, resulting in a dataset of 3,248 East Asian individuals. SNPs with <99% genotyping success rates, with minor allele frequencies lower than 0.01, or with Hardy Weinberg equilibrium *P*-values lower than 1×10^{-7} were excluded. Additionally, exomic sequencing data of 1,208 Japanese individuals from five institutes, including Kyoto University, National Research Institute for Child Health and Development, Tohoku University, The University of Tokyo, and Yokohama City University, were available in this database. Exomic sequencing data were obtained using commercially available oligonucleotide libraries followed by applications to next-generation sequencers HiSeq1000 (Illumina),

77 HiSeq2000 (Illumina), and SOLiD 5500XL (Thermo Fisher Scientific, Waltham, MA, USA)).
78 The genotypes of rs13278062 were obtained on the basis of the whole-genome SNP
79 genotyping results, whereas the genotypes of rs6061548 were not available in this database.
80
81 ***Yokohama City University dataset***
82 The Yokohama City University dataset includes 1,048 Japanese healthy controls recruited
83 from the Yokohama City University, Okada Eye Clinic, and Aoto Eye Clinic in Yokohama,
84 Kanagawa Prefecture, Japan. Genotypes of samples from Yokohama City University were
85 determined using BeadChip DNA arrays, namely Human OmniExpress chip (Illumina), with
86 the standard protocol recommended by each manufacturer. Samples with a call rate less than
87 97% were excluded. SNPs were excluded based on the following quality control criteria: call
88 rate <98%; the rates of missing data were significantly different between cases and controls
89 ($P < 1.0 \times 10^{-6}$); overall minor allele frequency <1%; and significant deviation from
90 Hardy-Weinberg equilibrium in controls ($P < 1.0 \times 10^{-5}$). Additionally, cryptic relatedness
91 between samples was estimated based on identity by descent; closely related samples with a
92 pi-hat >0.1875 were eliminated. Finally, 556,905 autosomal SNPs (1,048 controls) on the
93 Illumina Human OmniExpress chip that passed the filters were used for subsequent
94 imputation analyses. The Michigan imputation server
95 (https://imputationserver.sph.umich.edu/index.html#!pages/home) with the 1000 Genomes

dataset (phase3 v5 release) was used as a reference panel. All imputed SNPs were filtered with the quality control parameters (minor allele frequency >0.01 and squared correlation between imputed and true genotypes [r^2] > 0.7).

Replication stage 2 (Kobe CSC case-control dataset)

The details of this dataset are described elsewhere.[7] Briefly, individuals with idiopathic CSC recruited at Kobe University Hospital and population-based volunteers recruited by Kyushu University were used. Patients with idiopathic CSC, which represents central serous retinal detachment without subretinal hemorrhage or suspected choroidal neovascularization in ICGA or OCT, were included. Patients administered corticosteroid therapy, whose central choroidal thickness was less than 250 μm, who were aged over 80 years, and those with past histories of retinal vessel occlusion or uveitis were excluded. No ophthalmic evaluations were performed in control samples. Genotypes of samples were determined using BeadChip DNA arrays, namely Human Omni Express BeadChips (Illumina). Strand check and flipping to forward strand were performed using conform-gt (https://faculty.washington.edu/browning/conform-gt.html), the utility program for BEAGLE 4.1. Genotype data of 1000 Genomes CHB and JPT (The 1000 Genomes Project Consortium 2015a and 2015b) were used as references for the strand check procedure. Imputation was performed using BEAGLE 4.1 with genotype data of 1000 Genomes phase 3

(http://bochet.gcc.biostat.washington.edu/beagle/1000_Genomes_phase3_v5a/) as a reference panel. SNPs with an allelic R^2 lower than 0.8, call rate <95%, minor allele frequency <1% or significant deviation ($P < 1.0 \times 10^{-5}$) from Hardy–Weinberg equilibrium were excluded. Samples with a call rate <90% or pi-hat value > 0.25 were excluded from further analyses. Finally, 6,598,085 SNPs from 137 CSC samples and 1,153 controls were included in the dataset.

Replication stage 3 (Caucasian CSC case-control dataset)

The details of this dataset are described elsewhere.[8] Briefly, European patients with chronic CSC recruited from outpatient clinics at the Radboud University Medical Centre (N = 307), University Hospital of Cologne (N = 71), and Leiden University Medical Center (N = 143) were included. Patients included in this study showed the presence of serous fluid on optical coherence tomography in either eye, RPE irregularities with 1 or more hot spots of leakage on fluorescein angiography in either eye, and corresponding hyper fluorescence on indocyanine green angiography. Patients in whom evidence of another explanatory diagnosis or complication was present were excluded from this study. Controls were obtained from the Nijmegen Biomedical Study (NBS), a population-based survey conducted by the Department for Health Evidence and the Department of Laboratory Medicine of the Radboudumc. In the NBS, 21,756 randomly selected age- and gender-stratified inhabitants of the municipality of

Nijmegen were invited to complete a postal questionnaire on, e.g., lifestyle and medical history, and to donate an 8.5-mL blood sample in a serum separator tube and a 10-mL EDTA blood sample. In this population-based study, no ophthalmologic grading was performed.

Genotypes of 521 CSC patients were obtained using OmniExpress-12 or OmniExpress-24chip, and 3,577 controls for which genotyping was available on the Omni The express platform was included in the analysis. Quality control steps were applied to the separate batches using PLINK software. Samples with a call rate of <97% were removed. In each batch, SNPs with genotype call rates <98% or showing deviations from Hardy-Weinberg equilibrium ($P < 10^{-6}$) were excluded and only variants with a MAF >1% were retained. Only variants with a call rate >98% in the full dataset were preserved, leaving 589,487 autosomal and 13,282 X-chromosomal variants that could be used for downstream analysis. To assess population stratification, the dataset was merged with the Hapmap3 data on individuals of known genetic ancestry. Data were pruned with a window size of 50 kb, step size of 5, and variance inflation factor of 2; principal component analysis was performed with PLINK. Only individuals of European ancestry were retained for further analysis. Cryptic relatedness within the dataset was analyzed with KING (v2.0). A kinship coefficient threshold of <0.0884 was used to remove duplicates and individuals with a first or second-degree relationship from the dataset. After quality control, a total of 589,487 autosomal and 13,282 X-chromosomal

variants were used to impute the dataset. Autosomal genotype data were phased using Eagle (v2.3), while the X chromosome was phased with ShapeIT (v2. r790). After phasing, the data were imputed with the Haplotype Reference Consortium release 1.1.2016 using the Michigan Imputation server (https://imputationserver.sph.umich.edu). SNPs were filtered on an imputation quality score of $R^2 > 0.3$ for common variants (MAF >5 %) and a $R^2 > 0.8$ for low frequency variants (MAF < 5%).

Expression of genes in human tissue

The Eyeintegration database (https://eyeintegration.nei.nih.gov/, v1.01) revealed that *TNFRSF10A* and *GATA5* are expressed in other human tissues (http://eyeIntegration.nei.nih.gov/?Dataset=Gene_2019&ID=TNFRSF10A,GATA5&Tissue=_Adipose_-_Subcutaneous_,_Adipose_-_Visceral_(Omentum)_,_Adrenal_Gland_,_Artery_-_Aorta_,_Artery_-_Coronary_,_Artery_-_Tibial_,_Bladder_,_Brain_-_Amygdala_,_Brain_-_Anterior_cingulate_cortex_(BA24)_,_Brain_-_Caudate_(basal_ganglia)_,_Brain_-_Cerebellar_Hemisphere_,_Brain_-_Cerebellum_,_Brain_-_Cortex_,_Brain_-_Frontal_Cortex_(BA9)_,_Brain_-_Hippocampus_,_Brain_-_Hypothalamus_,_Brain_-_Nucleus_accumbens_(basal_ganglia)_,_Brain_-_Putamen_(basal_ganglia)_,_Brain_-_Spinal_cord_(cervical_c-1)_,_Brain_-_Substantia_nigra_,_Breast_-_Mammary_Tissue_,_Cells_-_EBV-transformed_lymphocytes_,_Cells_-_Leukemia_cell_line_(CML)_,_Cervix_-_Ectocervix_,_Cells_-_Transformed_fibro

blasts_,_Cervix_-_Endocervix_,_Colon_-_Sigmoid_,_Colon_-_Transverse_,_Esophagus_-_Gastroesophageal_Junction_,_Esophagus_-_Mucosa_,_Esophagus_-_Muscularis_,_Fallopian_Tube_,_Heart_-_Atrial_Appendage_,_Heart_-_Left_Ventricle_,_Kidney_-_Cortex_,_Liver_,_Lung_,_Minor_Salivary_Gland_,_Muscle_-_Skeletal_,_Nerve_-_Tibial_,_Ovary_,_Pancreas_,_Pituitary_,_Prostate_,_Skin_-_Not_Sun_Exposed_(Suprapubic)_,_Skin_-_Sun_Exposed_(Lower_leg)_,_Small_Intestine_-_Terminal_Ileum_,_Spleen_,_Stomach_,_Testis_,_Thyroid_,_Uterus_,_Vagina_,_Whole_Blood_,Choroid_Plexus_-_Adult_Tissue,Cornea_-_Adult_Tissue,Cornea_-_Cell_Line_Endothelium,Cornea_-_Endothelium,Cornea_-_Fetal_Endothelium,Cornea_-_Limbus,Cornea_-_Stem_Cell_Endothelium,Cornea_-_Stroma,ESC_-_Stem_Cell_Line,EyeLid_-_Adult_Tissue,Lens_-_Stem_Cell_Line,Retina_-_3D_Organoid_Stem_Cell,Retina_-_Adult_Tissue,Retina_-_Adult_Tissue_AMD_MGS_2,Retina_-_Adult_Tissue_AMD_MGS_3,Retina_-_Adult_Tissue_AMD_MGS_4,Retina_-_Adult_Tissue_MGS_1,Retina_-_Fetal_Eye,Retina_-_Fetal_Tissue,Retina_-_RGC_Stem_Cell,Retina_Fetal_Tissue,Retinal_Endothelium_-_Adult_Tissue,RPE_-_Adult_Tissue,RPE_-_Cell_Line,RPE_-_Fetal_Tissue,RPE_-_Stem_Cell_Line&num=2, accessed 7 October 2019).

References

1. Aung, T. *et al.* A common variant mapping to CACNA1A is associated with susceptibility to exfoliation syndrome. *Nat. Genet.* **47,** 387-392 (2015).

2. Kuriyama, S. *et al.* The Tohoku medical megabank project: Design and mission. *J. Epidemiol.* **26,** 493-511 (2016).

3. Yamaguchi-Kabata, Y. *et al.* iJGVD: an integrative Japanese genome variation database based on whole-genome sequencing. *Hum. Genome Var.* **2,** 15050 (2015).

4. Nagasaki, M. *et al.* Rare variant discovery by deep whole-genome sequencing of 1,070 Japanese individuals. *Nat. Commun.* **6,** 8018 (2015).

5. Higasa, K. *et al.* Human genetic variation database, a reference database of genetic variations in the Japanese population. *J. Hum. Genet.* **61,** 547-553 (2016).

6. Narahara, M. *et al.* Large-scale East-Asian eQTL mapping reveals novel candidate genes for LD mapping and the genomic landscape of transcriptional effects of sequence variants. *PLoS One* **9,** e100924 (2014).

7. Miki, A. *et al.* Genome-wide association study to identify a new susceptibility locus for central serous chorioretinopathy in the Japanese population. *Investig. Opthalmology Vis. Sci.* **59,** 5542 (2018).

8. Schellevis, R. L. *et al.* Role of the complement system in chronic central serous chorioretinopathy: a genome-wide association study. *JAMA Ophthalmol.* (2018). doi:10.1001/jamaophthalmol.2018.3190

Supplementary Table 1. Description and test statistics of top 10 pathways from pathway analysis using VEGAS2

Pathway ID	Pathway length	Nominal *P* value	Empirical *P* value	Genes
M00412_ESCRT-III_complex	10	1.57×10^{-7}	2.60×10^{-5}	RNF103-CHMP3_CHMP2B_CHMP7_CHMP4C_CHMP5_CHMP4A_CHMP6_CHMP2A_CHMP4B
GO:0000920_cell_separation_after_cytokinesis	16	2.19×10^{-7}	0.00012	RNF103-CHMP3_MITD1_PDCD6IP_CHMP2B_CHMP7_CHMP4C_CHMP5_CEP55_CHMP4A_VPS4A_CHMP1A_CHMP6_VPS4B_CHMP2A_CHMP4B
GO:0046755_viral_budding	23	7.90×10^{-7}	0.00031	RNF103-CHMP3_MITD1_PDCD6IP_CHMP2B_VTA1_VPS37D_VPS37A_CHMP7_CHMP4C_VPS28_CHMP5_LRSAM1_TSG101_VPS37B_CHMP4A_VPS4A_CHMP1A_CHMP6_VPS4B_MVB12A_CHMP2A_CHMP4B
GO:1902592_multi-organism_membrane_budding	23	7.90×10^{-7}	0.00033	RNF103-CHMP3_MITD1_PDCD6IP_CHMP2B_VTA1_VPS37D_VPS37A_CHMP7_CHMP4C_VPS28_CHMP5_LRSAM1_TSG101_VPS37B_CHMP4A_VPS4A_CHMP1A_CHMP6_VPS4B_MVB12A_CHMP2A_CHMP4B
GO:0036258_multivesicular_body_assembly	28	7.65×10^{-7}	0.0005	RNF103-CHMP3_STAM2_PDCD6IP_CHMP2B_VTA1_VPS37D_VPS37A_CHMP7_CHMP4C_VPS28_CHMP5_STAM_TSG101_VPS37B_VPS36_CHMP4A_RAB11A_VPS4A_IST1_CHMP1A_SNF8_CHMP6_HGS_VPS4B_MVB12A_CHMP2A_CHMP4B
GO:1902590_multi-organism_organelle_organization	23	7.90×10^{-7}	0.0005	RNF103-CHMP3_MITD1_PDCD6IP_CHMP2B_VTA1_VPS37D_VPS37A_CHMP7_CHMP4C_VPS28_CHMP5_LRSAM1_TSG101_VPS37B_CHMP4A_VPS4A_CHMP1A_CHMP6_VPS4B_MVB12A_CHMP2A_CHMP4B
GO:0045947_negative_regulation_of_translational_i	18	2.47×10^{-6}	0.00052	EIF2B3_TPR_EIF2B4_PAIP2B_EIF2AK3_EIF2B5_BANK1_PAIP2_EIF4EBP3_EIF2AK1_EIF3E_AGO2_EIF4EBP2_RBM4_EIF2S1_EIF2A

nitiation				K4_RARA_RPL13A
GO:0044803_multi-organism_membrane_organization	26	1.68×10^{-6}	0.00054	RNF103-CHMP3_MITD1_PDCD6IP_HYAL2_CHMP2B_VTA1_VPS37D_VPS37A_CHMP7_CHMP4C_VPS28_CHMP5_LRSAM1_TSG101_VPS37B_GAS6_CHMP4A_VPS4A_CHMP1A_CHMP6_VPS4B_MVB12A_PVRL2_CHMP2A_CHMP4B
R-HSA-162588_Budding_and_maturation_of_HIV_virion	22	2.30×10^{-6}	0.00058	RPS27A_CHMP3_PDCD6IP_CHMP2B_VTA1_VPS37D_VPS37A_CHMP7_CHMP4C_VPS28_CHMP5_TSG101_VPS37B_UBC_CHMP4A_VPS4A_CHMP6_NEDD4L_VPS4B_UBA52_CHMP2A_CHMP4B
GO:0036257_multivesicular_body_organization	29	1.18×10^{-6}	0.0006	RNF103-CHMP3_STAM2_PDCD6IP_CHMP2B_VTA1_VPS37D_VPS37A_CHMP7_CHMP4C_VPS28_CHMP5_STAM_TSG101_VPS37B_VPS36_CHMP4A_RAB27A_RAB11A_VPS4A_IST1_CHMP1A_SNF8_CHMP6_HGS_VPS4B_MVB12A_CHMP2A_CHMP4B

Supplementary Figure 2. Discovery and meta-analyses of rs13278062 and rs6061548 with CSC after genomic control correction.

SNP	rs13278062		rs6061548	
	Sample size	P value	Sample size	P value
Discovery GWAS (before GC correction)	3,460	5.94×10^{-7}	3,460	2.52×10^{-7}
Discovery GWAS (after GC corrected)	3,460	1.59×10^{-5}	3,460	8.34×10^{-6}
Meta-analysis (after GC correction)	14,574	6.29×10^{-12}	13,672	2.57×10^{-12}

Supplementary Table 3. Summary of the studied cohorts.

		CSC			Controls		
Stage	Ethnicities	Institutes	N	Genotyping platform	Institutes	N	Genotyping platform
Discovery GWAS	Japanese	Kyoto	610	Omni Express, Asian Screening Array	Aichi Cancer Center Research Institute, Hayashi Eye Hospital, Mizoguchi Eye Hospital, Oita, Ideta Eye Hospital, Shinjo Eye Clinic, Miyata Eye Hospital, Ozaki Eye Hospital, Kyoto, Nagahama City Hospital[1]	2,850	Human610-Quad BeatChip, Omni Express
Replication stage 1	Japanese	Kyoto, Kagawa, Yamanashi, Fukushima	288	TaqMan genotyping assay	Kyoto University,[5,6] Tohoku dataset,[2–4] Yokohama City University dataset	5,449	Omni Express
Replication stage 2	Japanese	Kobe datasets[7]	137	Omni Express	Kobe datasets[7]	1,153	Omni Express
Replication stage 3	Caucasian	Caucasian dataset (Nijmegen, Cologne, Leiden)[8]	521	Omni Express	Caucasian dataset (NBS)[8]	3,577	Omni Express

References

1. Aung, T. *et al.* A common variant mapping to CACNA1A is associated with susceptibility to exfoliation syndrome. *Nat. Genet.* **47,** 387-392 (2015).
2. Kuriyama, S. *et al.* The Tohoku Medical Megabank Project: design and mission. *J. Epidemiol.* **26,** 493-511 (2016).
3. Yamaguchi-Kabata, Y. *et al.* iJGVD: an integrative Japanese genome variation database based on whole-genome sequencing. *Hum. Genome Var.* **2,** 15050 (2015).
4. Nagasaki, M. *et al.* Rare variant discovery by deep whole-genome sequencing of 1,070 Japanese individuals. *Nat. Commun.* **6,** 8018 (2015).
5. Higasa, K. *et al.* Human genetic variation database, a reference database of genetic variations in the Japanese population. *J. Hum. Genet.* **61,** 547-553 (2016).
6. Narahara, M. *et al.* Large-scale East-Asian eQTL mapping reveals novel candidate genes for LD mapping and the genomic landscape of transcriptional effects of sequence variants. *PLoS One* **9,** e100924 (2014).
7. Miki, A. *et al.* Genome-wide association study to identify a new susceptibility locus for central serous chorioretinopathy in the Japanese population. *Investig. Ophthalmology Vis. Sci.* **59,** 5542 (2018).
8. Schellevis, R. L. *et al.* Role of the complement system in chronic central serous chorioretinopathy: a genome-wide association study. *JAMA Ophthalmol.* (2018). doi:10.1001/jamaophthalmol.2018.3190

Supplementary Figures

Supplementary Figure 1: Quantile-quantile (QQ) plots from the discovery stage. QQ plots for the association between all analyzed single-nucleotide polymorphisms and CSC in the discovery stage. Each blue dot represents an observed statistic (defined as the -log10(P-value)) versus the corresponding expected statistic before genomic control, whereas each red dot represents the observed statistic versus the corresponding expected statistic after genomic control. The black line corresponds to the null distribution. The genomic inflation factor lambda (λ_{GC}) was 1.157.

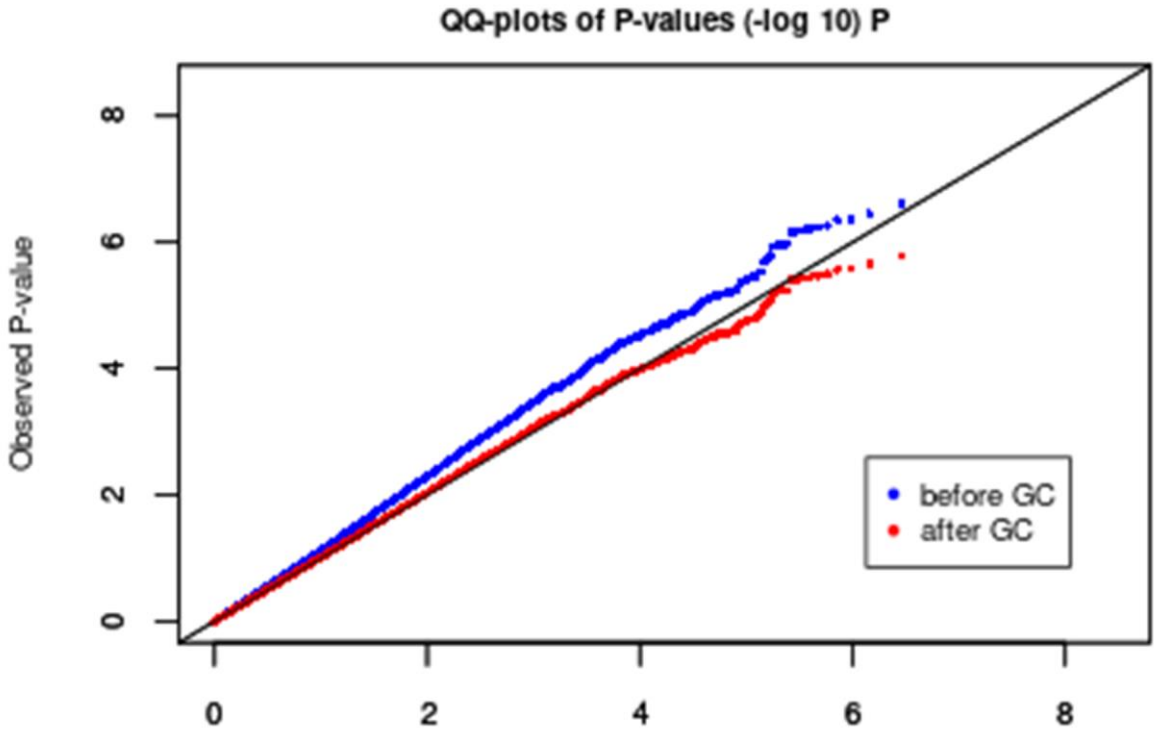

Supplementary Figure 2. Principal component analysis using five populations (AFR, SAS, EUR, EAS, JPT) from 1000 Genomes project and samples in the discovery GWAS (current study). The scatter plots for the first and second principal components.

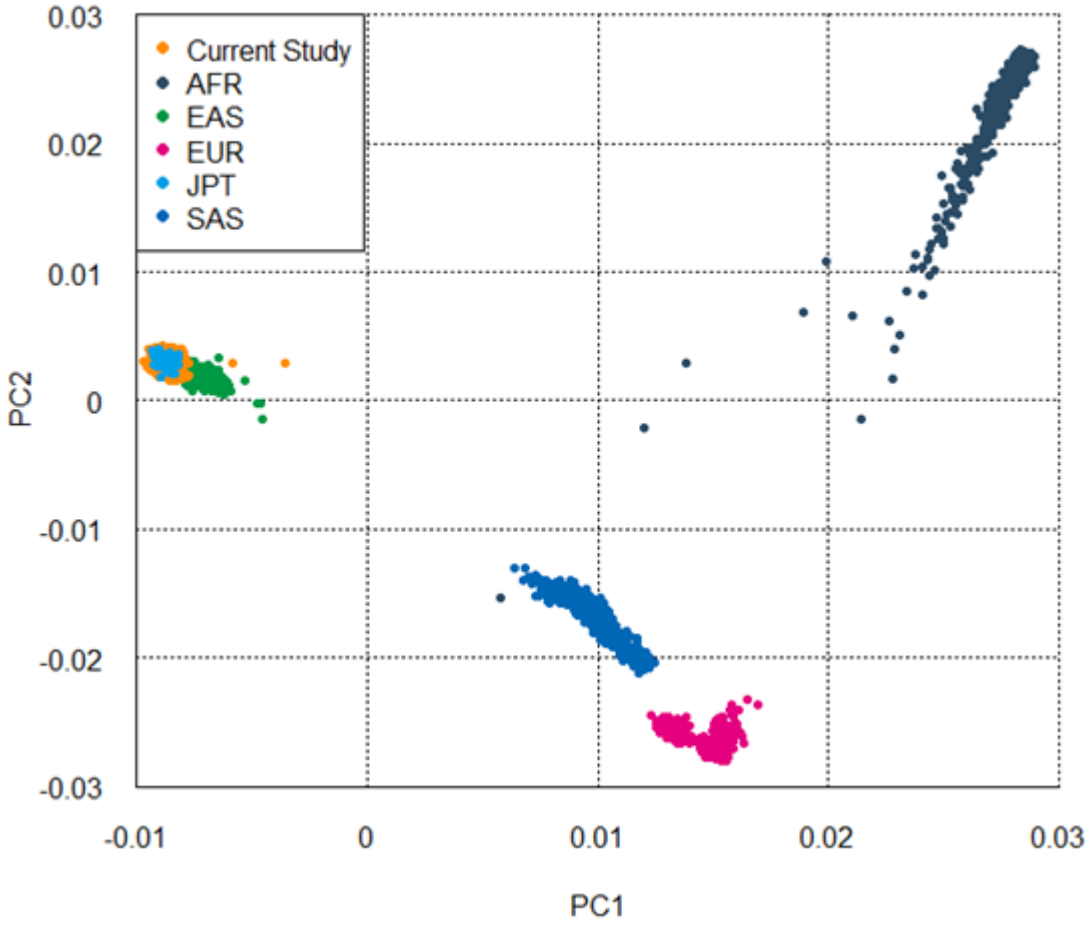

Supplementary Figure 3. Results of the principal component analysis using Japanese samples in the discovery GWAS. The scatter plots for the (A) first and second principal components, and (B) the second and third components.

Black and orange dots correspond to CSC and control samples, respectively.

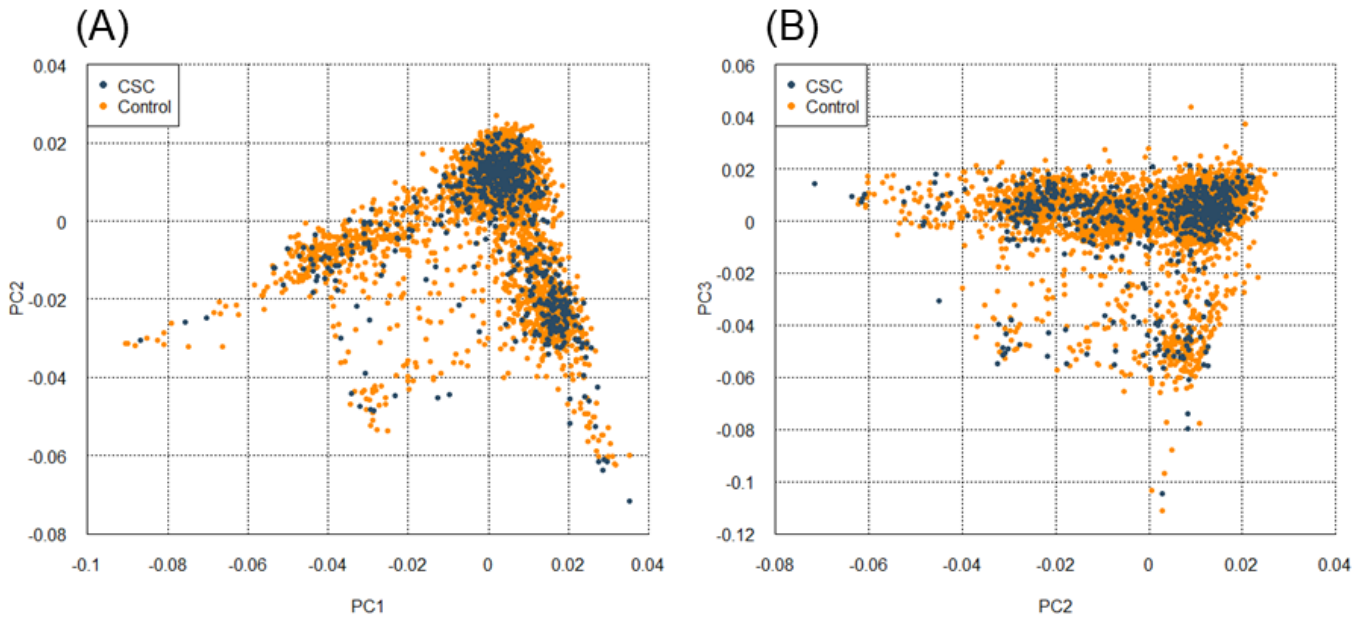

Supplementary Figure 4. Case-control association result and linkage disequilibrium (LD) map of the *TNFRSF10A-LOC389641* region.

LD block was defined based on the confidence interval rule.

Plots represent the −log10(P-values) obtained from the first-stage GWAS. The LD map based on R^2 values was drawn using genotype data of the cases and controls in GWAS samples.

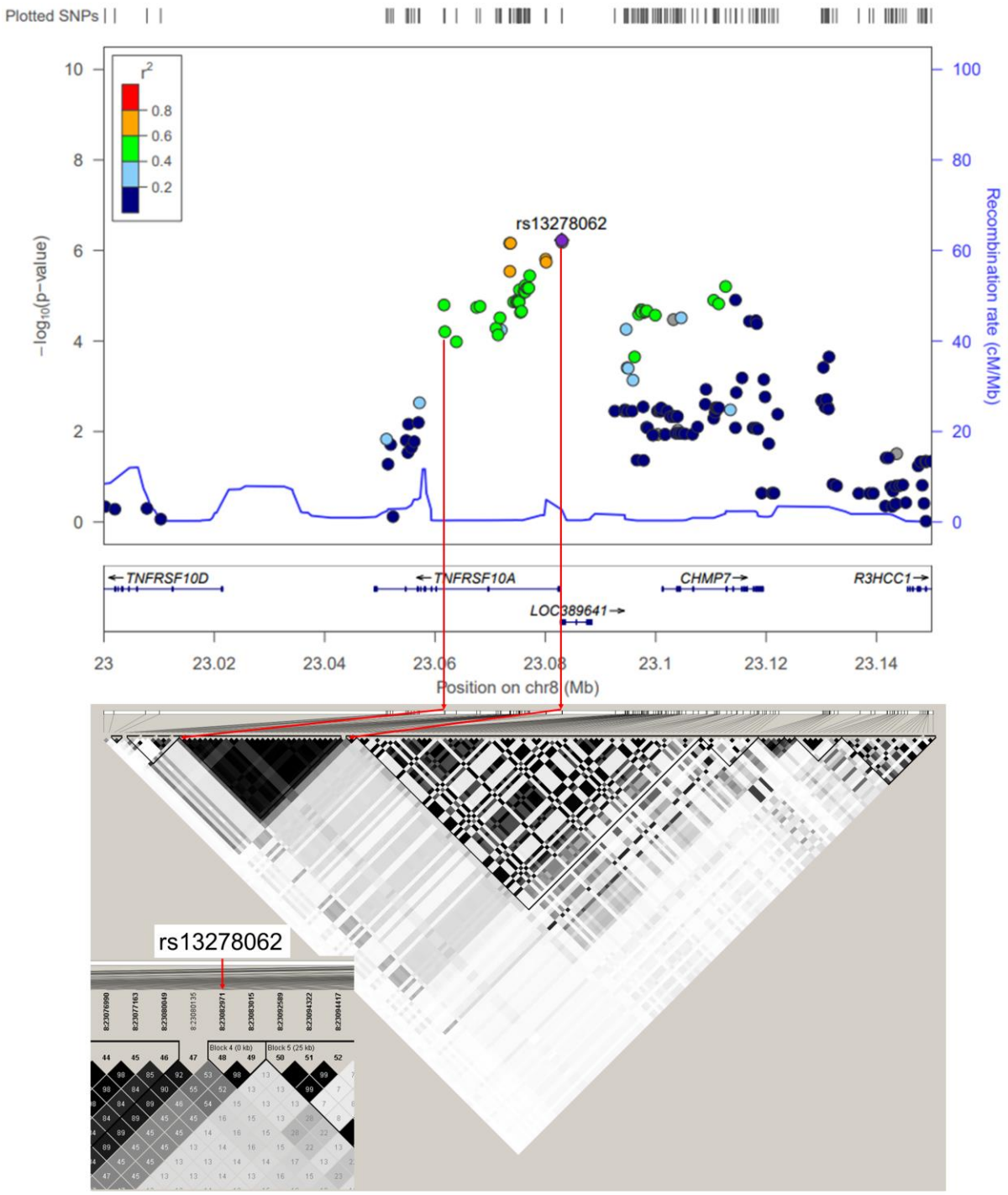

Supplementary Figure 5: Regional association plots around *GATA5* regions using GWAS data without quality control.

A strong signal is observed within the *GATA5* region; rs13044490 exceeded the genome-wide significance threshold ($P = 2.94 \times 10^{-10}$). The odds ratio for the occurrence of CSC was 1.67 (95% confidence interval, 1.42–1.95).

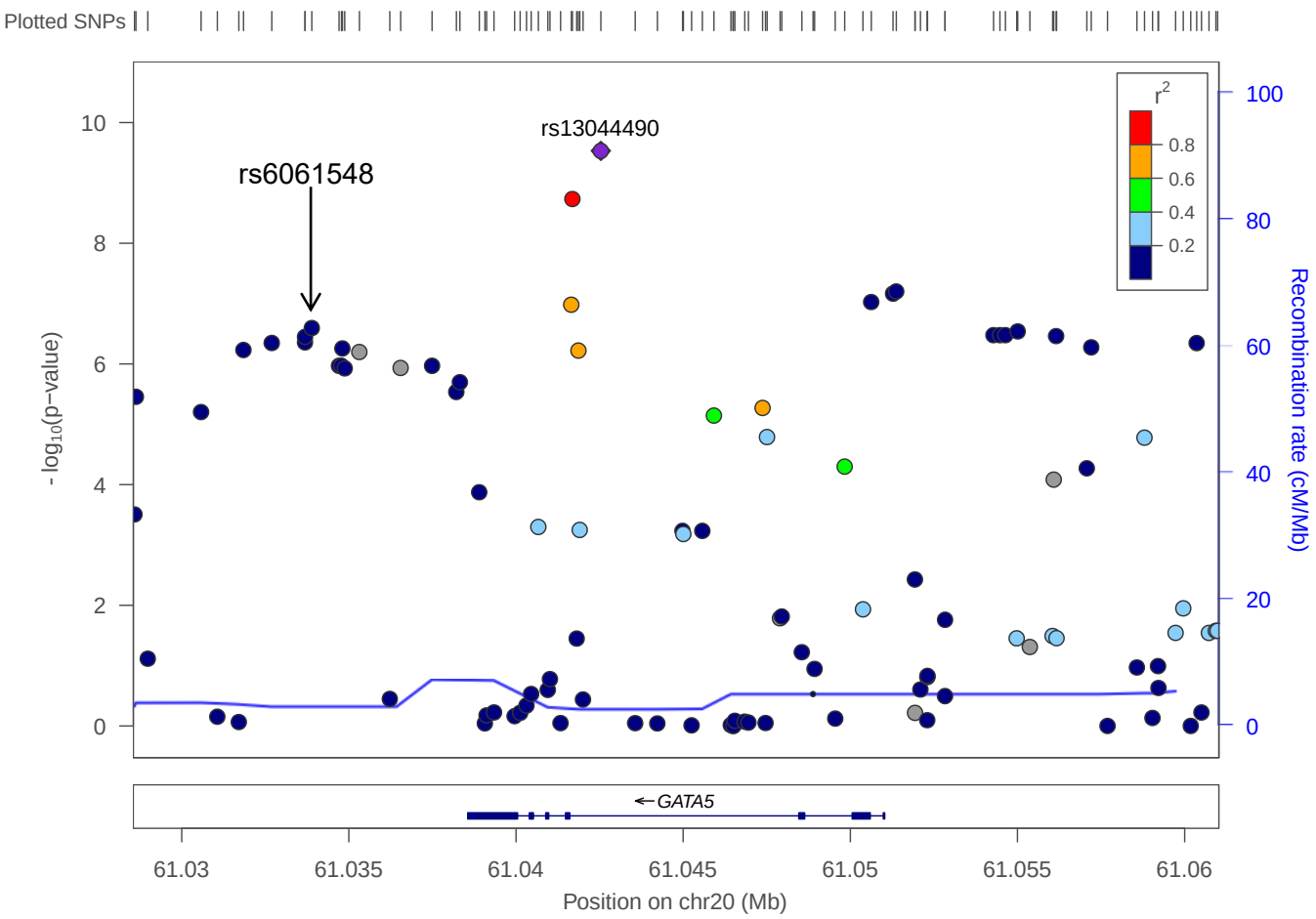

Supplementary Figure 6. Multi-tissue eQTL comparison of association between rs13278062 and *TNFRSF10A* expression.

Multi-tissue eQTL plot from publicly available quantitative trait locus analysis (eQTL) database search (GTEx Portal. https://gtexportal.org/home/) is shown. The effect size of rs13278062 on *TNFRSF10A* expression was strongest in the adrenal gland (normalized effect size = -0.973, $P = 4.5 \times 10^{-39}$), followed by the aorta (normalized effect size = -0.827, $P = 1.6 \times 10^{-44}$).

Supplementary Figure 7. Multi-tissue eQTL comparison of association between rs13044490 and *GATA5* expression.

Multi-tissue eQTL plot from publicly available quantitative trait locus analysis (eQTL) database search (GTEx Portal. https://gtexportal.org/home/) is shown. The effect size of rs13044490 on *GATA5* expression was the strongest in sun-exposed skin (normalized effect size = 0.353, $P = 3.8 \times 10^{-7}$) and esophageal muscularis (normalized effect size = 0.347, $P = 3.9 \times 10^{-8}$).